Terahertz conductivity at the Verwey transition in magnetite

A. Pimenov, S. Tachos, T. Rudolf, and A. Loidl
Experimentalphysik V, EKM, Universität Augsburg, 86135 Augsburg, Germany

D. Schrupp, M. Sing, and R. Claessen
Experimentalphysik II, Universität Augsburg, 86135 Augsburg, Germany

V. A. M. Brabers
Department of Physics, Eindhoven University of Technology, NL-5600, MB Eindhoven, The Netherlands
(Received 25 March 2005; published 29 July 2005)

The complex conductivity at the (Verwey) metal-insulator transition in Fe_3O_4 has been investigated at terahertz and infrared frequencies. In the insulating state, both the dynamic conductivity and the dielectric constant reveal a power-law frequency dependence, the characteristic feature of hopping conduction of localized charge carriers. The hopping process is limited to low frequencies only, and a cutoff frequency $\nu_1 \simeq 8$ meV must be introduced for a self-consistent description. On heating through the Verwey transition the low-frequency dielectric constant abruptly decreases and becomes negative. Together with the conductivity spectra this indicates the formation of a narrow Drude peak with a characteristic scattering rate of about 5 meV containing only a small fraction of the available charge carriers. The spectra can be explained assuming the transformation of the spectral weight from the hopping process to the free-carrier conductivity. These results support an interpretation of Verwey transition in magnetite as an insulator-semiconductor transition with structure-induced changes in activation energy.

DOI: 10.1103/PhysRevB.72.035131 PACS number(s): 71.30.+h, 78.30.−j, 78.70.Gq

I. INTRODUCTION

Magnetite (Fe_3O_4) is probably the oldest known magnetic material that can be found in natural form. This material is of considerable importance because of various applications in magnetic recording and for high-frequency electronic devices. Physical properties of magnetite have attracted much attention after the discovery of the first-order metal-insulator transition at $T_V \sim 120$ K. On cooling through the transition temperature, the dc conductivity drops by two orders of magnitude. A realistic model to explain the mechanism of this transition has been suggested by Verwey,[1] assuming a charge order-disorder transition with alternating valence (Fe^{2+}/Fe^{3+}) of the octahedrally coordinated iron ions. The metal-to-insulator transition in magnetite has been termed the Verwey transition since then. In spite of a large number of experimental and theoretical efforts, the mechanism governing the conduction and magnetic properties in magnetite is still under debate.[2,3] According to the results of recent x-ray resonant scattering,[4] even the charge ordering below T_V has been questioned, and the concept of an itinerant magnet was considered instead. Also, the importance of the orbital degrees of freedom has recently been highlighted.[5]

Magnetite crystallizes in a cubic high-temperature structure and exhibits a monoclinic distortion below the Verwey transition. In spite of enormous progress in resolving the low-temperature monoclinic structure of magnetite,[6–8] full details could not be completely resolved so far. The monoclinic phase is insulating and is characterized by a gap of the order of 100 meV in the excitation spectrum, which is seen in photoemission data,[9–11] in thermoelectric properties,[12] and by optical spectroscopy.[13,14] The charge transport in magnetite is usually explained within a polaronic picture.[13–16] However, there is no general agreement about the energy of the polaronic absorption in the conductivity spectra.[13–16] Recent photoemission results,[11] obtained in the same magnetite crystals as in the present paper, have been self-consistently explained using a small-polaron model. A similar concept has been applied recently to explain the dynamic conductivity at the metal-insulator transition in quasi-one-dimensional β-$Na_{0.33}V_2O_5$.[17]

At low temperatures the conduction in magnetite takes place via hopping between localized states, which agrees well with both activated dc resistivity[18–20] and with an observed characteristic power law $\sigma \propto \nu^s$ (Ref. 21) of the ac conductivity. This universal[22] power law has been observed in various materials with internal disorder and is a clear fingerprint of hopping of charge carriers.[23–25] The situation gets more complicated in the metallic state. In spite of two orders-of-magnitude increase in resistance above T_V, the absolute value of the dc conductivity $[\sigma_{dc}(T \gtrsim T_V) \sim 50\ \Omega^{-1}\,\mathrm{cm}^{-1}]$ is still much smaller than the Ioffe-Regel[26] minimum metallic conductivity $\sigma_{min} \sim e^2/3\hbar a \sim 3000\ \Omega^{-1}\,\mathrm{cm}^{-1}$, even including the Mott correction[27] in the case of the disorder $\sigma_{min} \sim 0.03 e^2/\hbar a \sim 300\ \Omega^{-1}\,\mathrm{cm}^{-1}$ (here $a \sim 3$ Å is the interatomic distance). The high-temperature conductivity of magnetite is thus typical for a semiconductor with a high mobility of thermally excited charge carriers rather than for a metal. Reviews of the recent and past developments in magnetite can be found in Refs. 2, 3, and 28–30.

In this paper we investigate terahertz (THz) and infrared conductivity of magnetite on both sides of the metal-to-insulator transition. The unexpected result of these experiments is the abrupt change of the dielectric constant at the

transition temperature yielding even negative values above T_V. Together with the conductivity spectra, these results indicate the formation of a narrow band of quasi-free carriers that contains only a small part of the total spectral weight.

II. EXPERIMENTAL DETAILS

Synthetic single crystals of magnetite were prepared from α-Fe_2O_3 using a floating-zone method with radiation heating.[31] Two single crystals were used for the measurements, which revealed slightly different transition temperatures, $T_V \simeq 123 \pm 1$ K and 116 ± 1 K, respectively. The transition temperature in magnetite can be taken as a criterium for impurity concentration and oxygen stoichiometry,[2,32] which, therefore, differ significantly for the two crystals investigated. Both samples revealed qualitatively similar electrodynamic properties, revealing only differences in absolute values. Therefore, in the following, mainly the results on a sample with $T_V \simeq 123$ K will be shown. Plane-parallel samples of different thicknesses between 0.5 and 0.05 mm have been prepared from the original boules. To ensure mechanical stability, the thinnest samples were glued onto a MgO substrate of $\simeq 0.5$ mm thickness. The availability of samples with different thicknesses is essential for transmittance experiments due to the strongly temperature-dependent absorption in magnetite.

The dynamic experiments for frequencies $4\ \mathrm{cm}^{-1} < \nu < 40\ \mathrm{cm}^{-1}$ were carried out in a Mach-Zehnder interferometer arrangement,[33] which allows both: the measurements of the transmittance and the phase shift of a plane-parallel sample. The complex transmission coefficient has been analyzed using the Fresnel optical formulas for transmittance $T=|t|^2$ of a plane-parallel sample:[34,35]

$$t = \sqrt{T} e^{i\phi_T} = \frac{(1-r^2)t_1}{1-r^2 t_1^2}, \tag{1}$$

where $r=(\sqrt{\varepsilon^*}-1)/(\sqrt{\varepsilon^*}+1)$ and $t_1=\exp(-2\pi i\sqrt{\varepsilon^*}d/\lambda)$. Here r is the reflection amplitude of a thick sample, t_1 is the "pure" transmission amplitude, ε^* is the complex dielectric permittivity of the sample, d is the sample thickness, and λ is the radiation wavelength. It has been assumed that the magnetic permeability $\mu=1$ in the frequency range of our experiments. The transmittance for a two-layer system can be obtained in a similar way.[34,35] Using Eq. (1), the absolute values of the complex conductivity $\sigma^*=\sigma_1+i\sigma_2$ and dielectric permittivity $\varepsilon^*=\varepsilon_1+i\varepsilon_2=\sigma^*/i\varepsilon_0\omega$ can be determined directly from the measured spectra. Here ε_0 and $\omega=2\pi\nu$ are the permittivity of vacuum and the angular frequency, respectively. In general, the phase shift ϕ_T in the transmittance experiment contains a possible ambiguity of $2\pi n$, where n is an integer. To exclude this source of errors, the reflectance of a thick sample has been measured in addition to the transmittance experiments. A similar Mach-Zehnder arrangement allowed us to obtain the amplitude and the phase shift of the reflectance at the Verwey transition. In total, a set of four measured quantities was available to calculate the real and imaginary part of the dynamic conductivity in the THz frequency range.

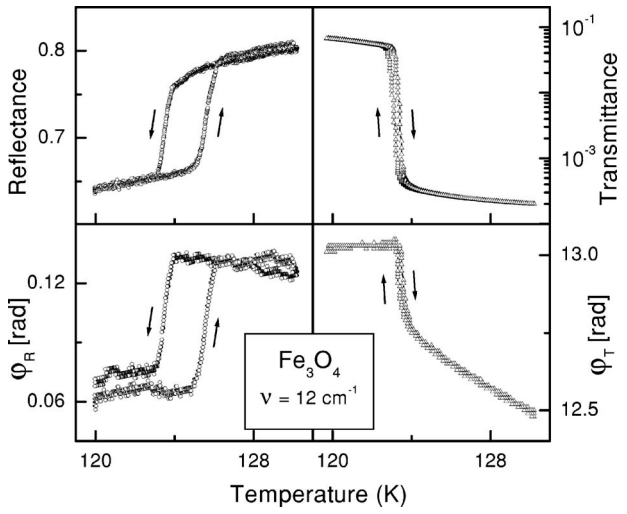

FIG. 1. Left panels: temperature-dependent reflectance (top left) and reflectance phase shift (bottom left) of magnetite at $\nu = 12\ \mathrm{cm}^{-1}$ in the vicinity of the Verwey transition. Right panels: transmittance (top) and phase shift (bottom) of a 0.05-mm-thick plane-parallel sample glued on the 0.5-mm-thick MgO substrate. The four measured quantities represent two data sets to determine σ_1 and $\varepsilon_1=-\sigma_2/\varepsilon_0\omega$.

In the infrared and visible frequency ranges $30\ \mathrm{cm}^{-1} < \nu < 21\,000\ \mathrm{cm}^{-1}$, the complex conductivity has been obtained via the Kramers-Kronig analysis of the reflectivity of the thick sample. The reflectivity experiment were performed using Bruker IFS-113v and IFS 66v/S Fourier-transform spectrometers. Different sources, beam splitters, and optical windows allowed us to cover the complete frequency range. In addition, the reflectance for the frequency range $4\ \mathrm{cm}^{-1} < \nu < 40\ \mathrm{cm}^{-1}$ has been calculated using the complex conductivity data, obtained by the transmittance technique described above. The combination of the results from two experimental techniques[36] substantially expands the low-frequency limit of the available spectrum and the quality of the subsequent Kramers-Kronig transformation.

III. RESULTS AND DISCUSSION

Figure 1 shows the complex reflectance and transmittance of magnetite in the vicinity of the Verwey transition. All four quantities reveal strong changes at the transition temperature. The most dramatic changes are observed in the transmittance, which decreases by three orders of magnitude. Both transmittance and reflectance show a hysteretic behavior, characteristic for a first-order phase transition. However, the experimentally observed hysteresis extends over different temperature regimes: the hysteresis spans $\Delta T \simeq 2$ K in the reflectance experiments, and is significantly less than 0.5 K in transmittance experiments. We suggest that this distinct difference probably results from the sample geometries, namely utilizing a thick sample ($\simeq 5$ mm) in the reflectance and thin sample ($\simeq 0.05$ mm) in the transmittance experiments. Except for the hysteresis region, all measurements revealed results coinciding within the experimental accuracy (Fig. 2). The effective overdetermination of the physical

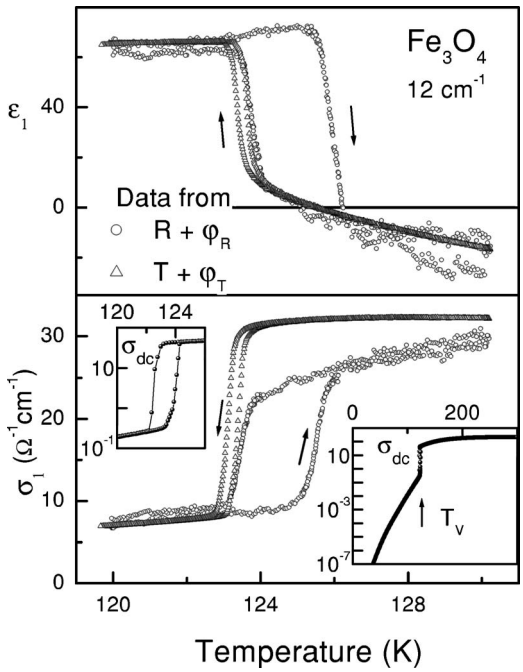

FIG. 2. Temperature dependence of the dielectric constant (ε_1, upper panel) and conductivity (σ_1, lower panel) in magnetite at $\nu = 12\ \mathrm{cm}^{-1}$. The data have been calculated from the complex reflectance (circles) of a thick sample and from the complex transmittance of a 0.05-mm-thin plate (triangles). Right inset: the dc conductivity of a thick sample in full temperature range; left inset: the temperature region close to the Verwey transition.

quantities, ε_1 and σ_1, in these experiments was necessary because of the highly unusual temperature and frequency dependence of the electrodynamic properties of magnetite (as discussed below).

Figure 2 shows the temperature dependence of the conductivity (σ_1) and the dielectric constant (ε_1) of magnetite at $\nu = 12\ \mathrm{cm}^{-1}$. The data have been obtained either from the complex transmittance [$t = \sqrt{T}\exp(i\phi_T)$, triangles] or from the complex reflectance [$r = \sqrt{R}\exp(i\phi_R)$, circles]. The conductivity reveals a sharp increase by a factor of 3 at the transition temperature. However, this value is substantially lower than the increase by two orders of magnitude, observed in the dc conductivity (insets of Fig. 2). This is a direct consequence of the power-law frequency dependence of the ac conductivity yielding an orders-of-magnitude increase of the conductivity with increasing frequency.

The behavior of the dielectric constant at the Verwey transition is highly unusual. Both transmittance and reflectance experiments lead to a strong *decrease* of the dielectric constant at the metal-to-insulator transition, becoming even negative above T_V. In the classical systems revealing a metal-to-insulator transition (e.g., doped silicon), it has been observed that the dielectric constant diverges approaching the transition temperature from the insulating side,[27,37] which has been termed *dielectric catastrophe*. In agreement with this picture and using the same technique as presented here, a strong increase of the dielectric constant at the metal-insulator transition has been observed in Sr-doped $LaMnO_3$ (Ref. 38) and recently in a magnetic field-induced transition in $Pr(Ca:Sr)MnO_3$.[39] We believe that the first-order character of the phase transition in magnetite interrupts the increase of the dielectric constant, observed at $T < T_V$ ($d\varepsilon/dT \simeq 1\ \mathrm{K}^{-1}$ at low frequencies). Instead, the dielectric constant of magnetite abruptly jumps to negative values at the "metallic" side of the transition.

Figure 3 shows the frequency dependence of the conductivity and dielectric constant in magnetite. Symbols at low frequencies represent the results of the transmittance experiments. Solid lines above 30 cm^{-1} have been obtained via the Kramers-Kronig analysis of the reflectance. The lower frame of Fig. 3 shows the frequency dependence of σ_1 above and below the Verwey transition. The low-frequency conductivity in the insulating state is dominated by a power law in frequency ($\sigma_1 \propto \nu^s$ with $s \sim 1.3$) with a temperature-dependent amplitude and a weak temperature-dependent frequency exponent. As mentioned in Sec. I, a power-law behavior of the conductivity is a characteristic feature of hopping conduction between localized states.[23–25] Previously, the frequency exponent $s \sim 0.7$ has been observed in magnetite at low temperatures and at kHz-frequencies,[21] a value typical for the ac conductivity in the audio-frequency range. Substantially higher values of the exponent are expected at higher frequencies. Approaching the phonon-assisted-hopping regime, $\sigma_1 \propto \nu^2$ has been predicted for low temperatures.[40] The transition to higher frequency exponents in the microwave frequency range has been discussed recently for doped semiconductors.[41] The power-law term is generally referred to as the universal dielectric response[22] and has been a recent matter of discussion concerning a possible universal superlinear power law with $s \gtrsim 1$ at high frequencies.[42]

The frequency dependence of the dielectric constant in magnetite is shown in the upper panel of Fig. 3. The behavior of the dielectric constant in the insulating state agrees qualitatively with the power law of σ_1, i.e., ε_1 increases with decreasing frequency. For $s > 1$ the low-frequency behavior can be approximated by $\varepsilon_1(0) - \varepsilon_1(\nu) \propto \nu^{s-1}$.

The dashed lines in Fig. 3 for the insulating state ($T < T_V$) were obtained by fitting the experimental data to the expression

$$\sigma_1(\nu) = \sigma_{dc} + A\frac{(\nu/\nu_1)^s}{1 + (\nu/\nu_1)^4}. \tag{2}$$

Here σ_{dc} is the dc conductivity and A is the amplitude of the hopping process. Compared to the conventional form of this response,[22–25,42] we introduced an additional high-frequency cutoff $[1 + (\nu/\nu_1)^4]$. The cutoff frequency ν_1 only weakly influences the conductivity in the low-frequency range but prevents the divergence of the spectral weight of $\sigma_1 \propto \nu^s$ at high frequencies.

The analytical expression for the dielectric constant has been obtained by applying the Kramers-Kronig transformation[43] to Eq. (2), which gives the following analytical expression for the dielectric constant:

$$\varepsilon_1(\nu) = \frac{\sigma_1(\nu) - \sigma_{dc}}{2\pi\nu\varepsilon_0}\left\{\tan(s\pi/2) - \frac{(\nu/\nu_1)^{1-s}}{\cos(s\pi/2)}\left[\sin\left((s+1)\frac{\pi}{4}\right) + \left(\frac{\nu}{\nu_1}\right)^2\cos\left((s+1)\frac{\pi}{4}\right)\right]\right\}. \tag{3}$$

This expression is valid both for $s < 1$ and for $s > 1$.

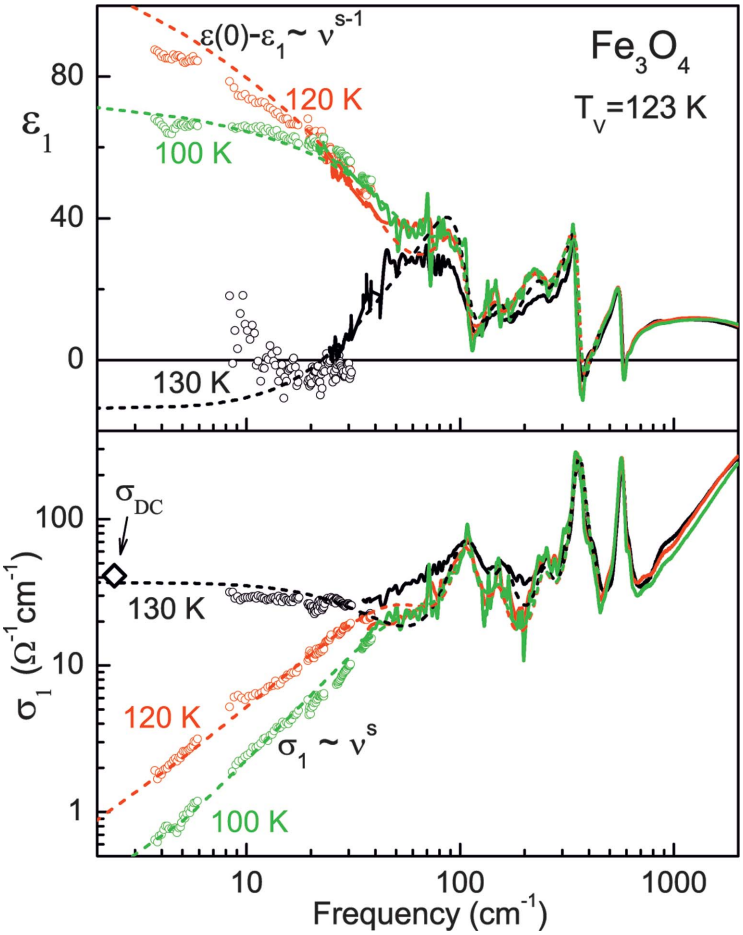

FIG. 3. (Color) Frequency dependence of the conductivity (σ_1, lower panel) and the dielectric constant (ε_1, upper panel) of magnetite above and below $T_V \simeq 123$ K. Symbols below 40 cm^{-1} and solid lines above 30 cm^{-1} represent the experimental data; dashed lines are the model calculations. Experimental data have been obtained from transmittance and phase shift of a thin Fe_3O_4 plate below 40 cm^{-1}, and via the Kramers-Kronig analysis of the reflectance of the thick sample above 30 cm^{-1}. The main contribution to the model calculations is given by the hopping term [$\sigma^* \propto \nu^s$, Eq. (2)] below T_V and a Drude term [Eq. (4)] above T_V.

To take into account the phononic and high-frequency electronic contributions, the sum of six Lorentzians has been added to expressions Eq. (2) and Eq. (3). Five Lorentzians at frequencies of 106, 152, 247, 361, and 574 cm^{-1} represent phonon contributions. An additional overdamped oscillator at 4270 cm^{-1} (0.53 eV) approximates the first excitation of the electronic origin. The given characteristic frequencies agree well with the published data.[13–15] In order to simplify the analysis of the THz conductivity and obtain the essential physics of the problem, the contributions from the Lorentzians were fixed for all three temperatures in Fig. 3. The parameters obtained from simultaneous fitting of the conductivity and dielectric constant are given in Table I.

A remarkable feature of the parameters for the low-temperature insulating phase in Table I is the low value of the cutoff frequency ν_1. Indeed, a qualitative examination of the conductivity frame of Fig. 3 reveals that the hopping process $\sigma_1 \propto \nu^s$ and the low-frequency edge of the electronic excitation ($\nu > 1000$ cm^{-1}) are well separated in energy. This indicates that the cutoff frequency of the hopping must be in the range $\sim$100 cm^{-1}, in agreement with the fits. This result is rather surprising and suggests that the low-temperature conductivity is governed by phonons.

In contrast to the gradual variation of $\varepsilon_1(\omega,T)$ and $\sigma_1(\omega,T)$ at low temperatures, dramatic changes are observed at the Verwey transition. At low frequencies the conductivity increases by more than one order of magnitude. This increase is substantially smaller than a change of two orders of magnitude in dc conductivity (see insets of Fig. 2). This difference is the result of a power-law frequency dependence of the conductivity in the insulating state. As a consequence, for frequencies close to 35 cm^{-1} we observe almost *no conductivity change* at T_V. This observation has been verified in a separate temperature-dependent experiment at $\nu = 35$ cm^{-1} (not shown).

As discussed above, the decrease of the dielectric constant at the transition to the conducting state is not expected within the scope of a conventional metal-insulator transition scenario. In order to find an explanation to this experimentally observed behavior, we mention that a negative dielectric con-

TABLE I. Parameters of the THz-frequency excitations in magnetite close to the Verwey transition that correspond to Eqs. (2)–(4). The changes in conductivity can be well described assuming the transformation of the hopping term Eq. (2) into the Drude term Eq. (4) with a high mobility of the quasi-free carriers.

T (K)	ν_1 (cm^{-1})	s	A (Ω^{-1} cm^{-1})
100	70	1.5	39
120	60	1.2	44
T (K)	$1/2\pi\tau$ (cm^{-1})		σ_{dc} (Ω^{-1} cm^{-1})
130	40		37

stant naturally follows by assuming a Drude response of quasi-free carriers,

$$\sigma^{*}_{DR} = \sigma_{dc}/(1 - i2\pi\nu\tau), \tag{4}$$

where σ_{dc} and $1/2\pi\tau$ are dc conductivity and the scattering rate, respectively. In addition to the negative changes in ε_1, the conductivity in the metallic state shows a slight downward curvature in the frequency dependence (lower panel of Fig. 3). This provides a further argument to include a Drude term to the model. Indeed, the simplest way to reproduce the experimental changes between 120 and 130 K is just to *replace* the hopping term [Eqs. (2) and (3)] by the Drude term. For the second sample of magnetite with $T_V \simeq 116$ K, a qualitatively similar behavior has been observed and the absolute values of the parameters agreed within ~20%. We believe that this variation partly corresponds to the difference in the conductivities of the samples.

The low value of the scattering rate, as observed in the present experiments, corresponds to a high carriers mobility of $\mu = e\tau/m \simeq 10^3$ cm^2/V s (assuming m being the free electron mass) and correlates well with the high quality of our magnetite single crystals. Due to the low characteristic frequency of the coherent (itinerant) process, its spectral weight,

$$S = \frac{2}{\pi}\int_0^{\infty} \sigma_{1,DR}(\omega)d\omega = \sigma_{dc}/\tau, \tag{5}$$

is small compared to the full number of carriers. Taking as an estimate of the total spectral weight the concentration of Fe^{2+} ions,[29] only about 2×10^{-4} of the theoretically available carriers participate in the coherent process. We recall further that within the rough estimate, the spectral weight of thermally activated quasi-free carriers in a semiconductor can be written as

$$S = \frac{ne^2}{m_{eff}} \exp\left(-\frac{\Delta_m}{k_B T}\right), \tag{6}$$

where n, e, and m_{eff} are concentration, charge, and effective mass of the charge carriers, respectively. In this expression the effective concentration of charge carriers is temperature activated and is governed by an energy gap Δ_m. The estimate of the effective mass $m_{eff} \simeq 10^2 m$ has been obtained from the infrared conductivity[14] and from the small-polaron analysis of photoemission of the same sample.[11] With this estimate for m_{eff} the observed small spectral weight of the Drude process corresponds to $\Delta_m \simeq 40$ meV, which correlates with a weakly activated dc conductivity just above T_V (right inset in Fig. 2). Within the same picture, the Verwey transition in magnetite corresponds just to an increase of the characteristic activation energy at the insulating side of the transition. The drop of dc conductivity at the transition can be ascribed to a gap change from $\Delta_m \simeq 40$ meV (conducting state) to $\Delta_i \simeq 90$ meV (insulating state). This new value of the energy gap agrees with the activation energy of dc conductivity,[18–20] thermoelectric power,[12] and with the gap values obtained in photoemission experiments.[9–11] The presented description implies the interpretation of the Verwey transition as an insulator-semiconductor transition with a change in activation energy induced by a crystal structure or by electronic configuration.

IV. CONCLUSIONS

Terahertz and infrared conductivity in magnetite has been obtained on both sides of the Verwey metal-to-insulator transition. Two orders of magnitude change in dc conductivity halves at millimeter frequencies and even disappear for $\nu \gtrsim 30$ cm^{-1}. In the far-infrared range, the effect of the transition remains solely in changing the dielectric constant (ε_1) of magnetite. The change of ε_1 during the transition into the conducting state is negative, which is in surprising contrast to an expected (positive) divergence of the dielectric constant at a metal-insulator transition. Within the simple model analysis the conductivity mechanism switches between the hopping of localized carries below T_V and itinerant motion above T_V. These results evidence the formation of the coherent state on the metallic side of the Verwey transition with high mobility of the charge carriers. Together with the recent photoemission data on the same samples, the interpretation of the Verwey transition as an insulator-semiconductor transition is suggested.

ACKNOWLEDGMENTS

The stimulating discussion with P. Lunkenheimer, L. V. Gasparov and I. Leonov is gratefully acknowledged. We thank A. A. Volkov, P. Pfalzer, and A. Pimenova for help in sample preparation, and S. Klimm for the measurement of the dc conductivity. This work was supported by BMBF (13N6917/0-EKM) and by DFG (SFB484-Augsburg).

[1] E. J. W. Verwey and P. W. Haayman, Physica (Amsterdam) **8**, 979 (1941); E. J. W. Verwey, P. W. Haayman, and F. C. Romeijn, J. Chem. Phys. **15**, 181 (1947).

[2] F. Walz, J. Phys.: Condens. Matter **14**, R285 (2002).

[3] J. García and G. Subías, J. Phys.: Condens. Matter **16**, R145 (2004).

[4] G. Subías, J. García, J. Blasco, M. Grazia Proietti, H. Renevier, and M. Concepción Sánchez, Phys. Rev. Lett. **93**, 156408 (2004); J. García, G. Subías, M. G. Proietti, J. Blasco, H. Renevier, J. L. Hodeau, and Y. Joly, Phys. Rev. B **63**, 054110 (2001).

[5] I. Leonov, A. N. Yaresko, V. N. Antonov, M. A. Korotin, and V. I. Anisimov, Phys. Rev. Lett. **93**, 146404 (2004).

[6] M. Iizumi, T. F. Koetzle, G. Shirane, S. Chikazumi, M. Matsui, and S. Todo, Acta Crystallogr., Sect. B: Struct. Crystallogr. Cryst. Chem. **38**, 2121 (1982).

[7] J. M. Zuo, J. C. H. Spence, and W. Petuskey, Phys. Rev. B **42**, 8451 (1990).

[8] J. P. Wright, J. P. Attfield, and P. G. Radaelli, Phys. Rev. Lett. **87**, 266401 (2001); Phys. Rev. B **66**, 214422 (2002).
[9] A. Chainani, T. Yokoya, T. Morimoto, T. Takahashi, and S. Todo, Phys. Rev. B **51**, 17976 (1995).
[10] J.-H. Park, L. H. Tjeng, J. W. Allen, P. Metcalf, and C. T. Chen, Phys. Rev. B **55**, 12813 (1997).
[11] D. Schrupp, M. Sing, M. Tsunekawa, H. Fujiwara, S. Kasai, A. Sekiyama, S. Suga, T. Muro, V. A. M. Brabers, and R. Claessen, Europhys. Lett. **70**, 789 (2005).
[12] A. J. M. Kuipers and V. A. M. Brabers, Phys. Rev. B **14**, 1401 (1976).
[13] S. K. Park, T. Ishikawa, and Y. Tokura, Phys. Rev. B **58**, 3717 (1998).
[14] L. V. Gasparov, D. B. Tanner, D. B. Romero, H. Berger, G. Margaritondo, and L. Forró, Phys. Rev. B **62**, 7939 (2000).
[15] L. Degiorgi, P. Wachter, and D. Ihle, Phys. Rev. B **35**, 9259 (1987); A. Schlegel, S. F. Alvarado, and P. Wachter, J. Phys. C **12**, 1157 (1979).
[16] D. Ihle and B. Lorenz, J. Phys. C **18**, L647 (1985); **19**, 5239 (1986).
[17] C. Presura, M. Popinciuc, P. H. M. van Loosdrecht, D. van der Marel, M. Mostovoy, T. Yamauchi, and Y. Ueda, Phys. Rev. Lett. **90**, 026402 (2003).
[18] B. A. Calhoun, Phys. Rev. **94**, 1577 (1954).
[19] M. Matsui, S. Todo, and S. Chikazumi, J. Phys. Soc. Jpn. **42**, 1517 (1977).
[20] A. J. M. Kuipers and V. A. M. Brabers, Phys. Rev. B **20**, 594 (1979).
[21] Y. Akishige, T. Fukatsu, M. Kobayashi, and E. Sawaguchi, J. Phys. Soc. Jpn. **54**, 2323 (1985); M. Kobayashi, Y. Akishige, and E. Sawaguchi, *ibid.* **55**, 4044 (1986).
[22] A. K. Jonscher, *Dielectric Relaxation In Solids* (Chelsea Dielectrics, London, 1983).
[23] A. R. Long, Adv. Phys. **31**, 553 (1982).
[24] S. R. Elliott, Solid State Ionics **27**, 131 (1988).
[25] J. C. Dyre and T. B. Schrøder, Rev. Mod. Phys. **72**, 873 (2000).
[26] A. F. Ioffe and A. R. Regel, Prog. Semicond. **4**, 237 (1960).
[27] N. F. Mott, *Metal-Insulator Transitions* (Taylor & Francis, London, 1990), p. 35.
[28] J. Honig, in *Metallic and Nonmetallic States of Matter*, edited by P. P. Edwards and C. N. Rao (Taylor & Francis, London, 1985), p. 226.
[29] N. Tsuda, K. Nasu, A. Yanase, and K. Siratori, *Electronic Conduction in Oxides* (Springer, Berlin, 1991) p. 207.
[30] M. Imada, A. Fujimori, and Y. Tokura, Rev. Mod. Phys. **70**, 1039 (1998).
[31] V. A. M. Brabers, J. Cryst. Growth **8**, 26 (1971).
[32] V. A. M. Brabers, F. Walz, and H. Kronmüller, Phys. Rev. B **58**, 14163 (1998).
[33] G. V. Kozlov and A. A. Volkovs, in *Millimeter and Submillimeter Wave Spectroscopy of Solids*, edited by G. Grüner (Springer, Berlin, 1998), p. 51; A. A. Volkov, Yu. G. Goncharov, G. V. Kozlov, S. P. Lebedev, and A. M. Prochorov, Infrared Phys. **25**, 369 (1985).
[34] O. S. Heavens, *Optical Properties of Thin Solid Films* (Dover, New York, 1991).
[35] M. Born and E. Wolf, *Principles of Optics* (Pergamon, Oxford, 1986).
[36] A. Pimenov, A. Loidl, and S. I. Krasnosvobodtsev, Phys. Rev. B **65**, 172502 (2002).
[37] H. F. Hess, K. DeConde, T. F. Rosenbaum, and G. A. Thomas, Phys. Rev. B **25**, 5578 (1982); M. Capizzi, G. A. Thomas, F. DeRosa, R. N. Bhatt, and T. M. Rice, Phys. Rev. Lett. **44**, 1019 (1980).
[38] A. Pimenov, C. Hartinger, A. Loidl, A. A. Mukhin, V. Yu. Ivanov, and A. M. Balbashov, Phys. Rev. B **59**, 12419 (1999).
[39] D. Ivannikov *et al.* (unpublished).
[40] N. F. Mott and E. A. Davis, *Electronic Processes in Noncrystalline Materials* (Clarendon Press, Oxford, 1979).
[41] E. Helgren, N. P. Armitage, and G. Grüner, Phys. Rev. B **69**, 014201 (2004); M. Lee and M. L. Stutzmann, Phys. Rev. Lett. **87**, 056402 (2001).
[42] P. Lunkenheimer and A. Loidl, Phys. Rev. Lett. **91**, 207601 (2003).
[43] F. Wooten, *Optical Properties of Solids* (Academic, New York, 1972) p. 173.